THE JOURNAL OF BIOLOGICAL CHEMISTRY VOL. 285, NO. 40, pp. 31037–31045, October 1, 2010

Control of AmtB-GlnK Complex Formation by Intracellular Levels of ATP, ADP, and 2-Oxoglutarate*[S]

Received for publication, June 11, 2010, and in revised form, July 15, 2010 Published, JBC Papers in Press, July 18, 2010, DOI 10.1074/jbc.M110.153908

Martha V. Radchenko, Jeremy Thornton, and Mike Merrick[1]

From the Department of Molecular Microbiology, John Innes Centre, Norwich NR4 7UH, United Kingdom

P_{II} proteins are one of the most widespread families of signal transduction proteins in nature, being ubiquitous throughout bacteria, archaea, and plants. They play a major role in coordinating nitrogen metabolism by interacting with, and regulating the activities of, a variety of enzymes, transcription factors, and membrane transport proteins. The regulatory properties of P_{II} proteins derive from their ability to bind three effectors: ATP, ADP, and 2-oxoglutarate. However, a clear model to integrate physiological changes with the consequential structural changes that mediate P_{II} interaction with a target protein has so far not been developed. In this study, we analyzed the fluctuations in intracellular effector pools in *Escherichia coli* during association and dissociation of the P_{II} protein GlnK with the ammonia channel AmtB. We determined that key features promoting AmtB-GlnK complex formation are the rapid drop in the 2-oxoglutarate pool upon ammonium influx and a simultaneous, but transient, change in the ATP/ADP ratio. We were also able to replicate AmtB-GlnK interactions *in vitro* using the same effector combinations that we observed *in vivo*. This comprehensive data set allows us to propose a model that explains the way in which interactions between GlnK and its effectors influence the conformation of GlnK and thereby regulate its interaction with AmtB.

Ammonium (in this work, the term is used in a general sense to include both NH_4^+ and NH_3) is the preferred nitrogen source for *Escherichia coli* and is easily assimilated through the activities of either glutamate dehydrogenase or the glutamine synthetase/glutamate synthase cycle. Historically, it was considered that ammonium enters the cell by unfacilitated membrane diffusion, but later studies demonstrated facilitated diffusion through ammonia channel proteins that are present in all domains of life (1–3). *E. coli* AmtB, which is a high-affinity low-capacity ammonia channel (10–10,000 molecules/s) (4, 5), is the paradigm for the whole Amt protein family (3). Its three-dimensional structure reveals a stable homotrimer in which each monomer has a cleavable signal peptide, so the mature protein has 11 transmembrane helices with an extracytoplasmic N terminus and a cytoplasmic C terminus (5–7). Each subunit of AmtB has a narrow, predominantly hydrophobic, pore containing a number of highly conserved residues that play critical roles in periplasmic NH_4^+ binding, NH_4^+ deprotonation, and NH_3 translocation (5, 7–9).

In *E. coli* and most prokaryotes, the gene encoding AmtB (*amtB*) is in an operon together with a second gene (*glnK*) encoding a member of the P_{II} family (10). P_{II} proteins are one of the most widespread signal transduction proteins in nature (11). They play a major role in coordinating the regulation of nitrogen metabolism by interacting with, and regulating the activities of, a variety of enzymes, transcription factors, and membrane transport proteins. *E. coli* has two P_{II} proteins, GlnB and GlnK, and their homologs are commonly found in other bacteria (12). The conserved genetic linkage between *glnK* and *amtB* suggested a functional association between GlnK and AmtB (10), and indeed an increase in cellular nitrogen status leads to AmtB-GlnK association and consequent inactivation of AmtB (13, 14). Definitive evidence for *in vivo* complex formation between GlnK and AmtB was obtained by purification of the intact complex from the membrane fraction of *E. coli* cells that had been subjected to a prior ammonium shock (15). A series of subsequent studies in other bacteria supported the proposition that this interaction is conserved among prokaryotes (16–19).

Like all P_{II} proteins, GlnK is a homotrimer. Each subunit contains 112 amino acids and is a compact, cylindrically shaped molecule from which three long exposed loops (the T-loops) protrude. The T-loops are significantly conserved in sequence but are structurally very flexible. They are vital for P_{II} interactions with many of their targets and are also sites of reversible covalent modification (20). In addition to the T-loops, P_{II} proteins are also characterized by three lateral intersubunit clefts within which are two smaller loops (the B- and C-loops).

Functionally, *E. coli* GlnK can be regarded as a signal integrator that has two modes of signal perception. First, like many (but not all) P_{II} proteins, GlnK is subject to covalent modification through the action of the bifunctional enzyme (GlnD) that covalently modifies GlnK by uridylylation or deuridylylation of Tyr^{51} in the T-loop (20). GlnD activity is regulated by the cellular glutamine pool; hence, the modification state of GlnK reflects the cellular glutamine status. The second mode of signal perception by GlnK, which is apparently conserved in all P_{II} proteins, consists of the binding of effector molecules ATP, ADP, and 2-oxoglutarate (2-OG)[2] (12, 20, 21). X-ray crystal structures have shown that ATP or ADP binds in the lateral clefts between the subunits, where the B- and T-loops from one subunit and the C-loop from another contribute to a nucleo-

* This work was supported by the Biotechnology and Biological Sciences Research Council (United Kingdom).

[S] The on-line version of this article (available at http://www.jbc.org) contains supplemental Fig. S1.

[1] To whom correspondence should be addressed. Tel.: 44-1603-450749; Fax: 44-1603-450778; E-mail: mike.merrick@bbsrc.ac.uk.

[2] The abbreviations used are: 2-OG, 2-oxoglutarate; ITC, isothermal titration calorimetry.

tide-binding pocket (22, 23). The binding site for 2-OG, which is expected to be conserved in all P_{II} proteins, has been elusive. However, a recent crystal structure of *Azospirillum brasilense* GlnZ revealed that both ATP and 2-OG bind in the lateral clefts, where they participate in the coordination of a Mg^{2+} ion (24). This is consistent with the observation that MgATP binding to GlnB and GlnK of *E. coli* is synergistic with the binding of 2-OG (20, 21).

Complex formation between *E. coli* GlnK and AmtB provides an excellent model system in which to explore, at the molecular level, the way that effector ligands control the interaction of a P_{II} protein with its target. Deuridylylation of GlnK, as a consequence of ammonium shock, coincides with its membrane sequestration by AmtB (14). The *E. coli* AmtB-GlnK complex has a stoichiometry of 1:1, and all molecules of GlnK within the complex are fully deuridylylated (15). The crystal structure of the AmtB-GlnK complex revealed that ADP and not ATP is present in all three lateral clefts of GlnK and that 2-OG and Mg^{2+} ions are absent (23, 25). The conformation of the GlnK T-loop is also critical for AmtB-GlnK interaction, and it appears that ADP may be required to favor the extended T-loop conformation that facilitates successful complex formation (23, 24).

In vitro studies of ligand effects on the *E. coli* AmtB-GlnK complex showed that high levels of 2-OG play a critical role in complex dissociation (15). Studies of homologous AmtB-P_{II} complexes have also implicated 2-OG and the ATP/ADP ratio in the regulation of complex formation (16–19). However, although these various studies have given some indications as to the roles of effectors in regulating the interaction of GlnK with AmtB, it has not yet been possible to link such effects to metabolic changes within the cell or to conformational changes in GlnK.

In the work reported here, we determined the intracellular pools of ATP, ADP, and 2-OG in *E. coli* and established the relationship between those metabolites and cellular nitrogen status under conditions that promote either association or dissociation of the AmtB-GlnK complex. We also studied the influence of physiologically relevant concentrations of Mg^{2+}, ATP, ADP, and 2-OG on *in vitro* interactions between purified GlnK and AmtB. A combination of these *in vivo* and *in vitro* data allows us to propose a molecular mechanism whereby changes in intracellular effector pools control the ability of GlnK to regulate ammonium influx through AmtB.

EXPERIMENTAL PROCEDURES

Strains and Plasmids—The following strains of *E. coli* were used: ET8000 (*rbs lacZ*::IS1 *gyrA hutC*$_K$) (26), GT1000 (ET8000 Δ*glnKamtB*) (14), and JW3841 (ECK3863 *glnA*::Km) (27). ET8009 (ET8000 *glnA*::Km) was constructed by P1 transduction of the *glnA*::Km allele from strain JW3841 into ET8000. Construction and verification of "scar" strain ET8010 (ET8000 Δ*glnA*) were carried out using plasmid pCP20 (28). Plasmid pAD2 was expressed in GT1000 and used for His_6-AmtB-GlnK complex purification (15). Plasmid pJT25 in *E. coli* BL21(DE3)pLysS (29) was used for overexpression of GlnK. It was constructed by digesting plasmid pMODULES3 (15) with NdeI and PstI and ligating the resulting 338-bp *glnK* gene into expression vector pT7-7 (30).

Protein Quantification and Western Blotting—Whole cell extracts were prepared from overnight cultures of ET8000 grown in M9Gln medium (4) at 30 °C and assayed with Coomassie Plus™ protein assay reagent (Thermo Scientific) using an albumin standard (Thermo Scientific). Pure AmtB and GlnK at concentrations of 5, 10, 20, and 40 ng/lane and whole cell extracts at concentrations of 1, 2, 4, 8, 16, and 32 μg/lane were separated by SDS-PAGE on a 12.5% gel and analyzed by Western blotting as described (14). Proteins were detected using an appropriate primary antibody: anti-*E. coli* GlnK (31) or anti-*E. coli* AmtB (13) raised in rabbits. The ECL Plex Western blotting detection system (GE Healthcare), ECL Plex Cy5-labeled goat anti-rabbit IgG secondary antibody (GE Healthcare), an FLA-7000 fluorescent image analyzer (Fujifilm Life Science), and the Gene Tools v.3.06 image analysis system (Syngene) were used for protein quantification. Integration parameters were as follows: base-line correction method, lowest slope; base-line correction offset, yes; color filtration options, no filter; Savitsky-Golay smoothing order 2, width 3; type, absorption; and image dimensions, whole membrane filter. Final data were obtained from three independent experiments.

In Vivo AmtB-GlnK Complex Formation and Cell Fractionation—1-ml aliquots of membrane and cytoplasmic extracts were prepared from 120 ml of culture grown in M9Gln medium at 30 °C and subjected to ammonium shock by the addition of NH_4Cl to a final concentration of 50, 100, 200, or 300 μM for 30 s, 1 min, 2 min, 5 min, 10 min, and 15 min. Membrane and cytoplasmic fractions were prepared as described previously (14), and membrane fractions were subjected to two high-salt washes (600 mM NaCl) prior to analysis.

Analysis of Intracellular 2-OG—Overnight cultures grown in M9Gln medium at 30 °C were subjected to ammonium shock. Portions of cultures (8 ml) taken prior to ammonium shock and 30 s, 2 min, 3 min, 5 min, 10 min, and 15 min after ammonium shock were immediately filtered through 0.45-μm pore size membrane filters (25-mm diameter) with vacuum suction. Extracts for measurement of 2-OG were prepared as described previously (32). 2-OG concentrations were determined by fluorometric reactions (32) using an LS55 fluorescence spectrometer (PerkinElmer Life Sciences). Data are the result of three independent experiments. Effectors concentrations (nmol/mg of total cell protein) were converted to intracellular concentrations (mM) based on an intracellular volume of 6.6 μl/mg of total cell protein.

Analysis of in Vivo ATP and ADP Levels—Quantitative detection of ATP and ADP was based on luciferase-driven bioluminescence and was carried out using the ATP Bioluminescence Assay Kit HS II (Roche Applied Science) and a SpectraMax Gemini XS microplate spectrofluorometer (Molecular Devices). Overnight cultures were grown in M9Gln medium at 30 °C. Aliquots (1 ml) were taken prior to ammonium shock and 15 s, 30 s, 1 min, 2 min, 3 min, 5 min, 10 min, and 15 min after ammonium shock and frozen in liquid N_2. Cells were lysed according to the manufacturer's protocol, and the supernatant of each lysate was divided into two 50-μl aliquots. One aliquot, for ATP measurement, received 50 μl of buffer containing 200

mM triethanolamine (pH 7.6), 2 mM $MgCl_2$, 240 mM KCl, and 4.6 mM phosphoenolpyruvate. The second aliquot, for ADP measurement, received 50 μl of the same buffer containing 3 units/ml pyruvate kinase. All samples were incubated at 37 °C for 10 min, placed on ice, and analyzed immediately.

Purification of the AmtB-GlnK Complex—This was performed as described previously (15) with minor modifications. Before harvesting, the cells were subjected to a 10 mM ammonium chloride shock. AmtB-GlnK complex was eluted from a HisTrap HP 1-ml column (GE Healthcare).

Effects of 2-OG, ATP, and ADP on the AmtB-GlnK Complex—The stability of the AmtB-GlnK complex when treated with effectors was studied as described previously (15) with some modifications. To simulate the *in vivo* environment for each condition tested, physiologically relevant concentrations of all three effectors were added to the washing buffer. The washed fractions were collected after applying effectors, and the eluted fractions were loaded on 15% SDS-polyacrylamide gel and stained with Instant Blue (Expedeon Ltd.).

Purification of His_6-AmtB and GlnK Proteins—Both proteins were obtained by purifying the complex as described previously (15), immobilizing it on a HIS-Select spin column, and subsequently dissociating it using 600 mM NaCl.

Effects of 2-OG, ATP, and ADP on His_6-AmtB and GlnK Proteins—AmtB (400 μg) was immobilized on a HIS-Select spin column previously equilibrated with buffer A (50 mM Tris-HCl (pH 8.0), 100 mM NaCl, 10% (v/v) glycerol, 0.05% (w/v) *n*-dodecyl-*N*,*N*-dimethylamine *N*-oxide) containing 5 mM imidazole. The flow-through fraction was collected, and unbound proteins were removed by two washes with the same buffer. Three additional washes were carried out in buffer A containing 5 mM imidazole, 300 μg of GlnK protein, and physiologically relevant concentrations of effectors (see "Results"). As a control, buffer A containing 5 mM imidazole, 300 μg of GlnK protein, and 0.6 M NaCl was used. The molar ratio of AmtB to GlnK was ~1:3. A single column was used for each condition tested. Elution of His_6-AmtB or His_6-AmtB-GlnK complex was performed by the addition of buffer A containing 500 mM imidazole. The eluted fractions were analyzed on 15% SDS-polyacrylamide gel.

Isothermal Titration Calorimetry (ITC)—Experiments were performed in an iTC_{200} isothermal titration calorimeter (MicroCal) at 28 °C in a cell volume of 0.2 ml. GlnK solutions (60–120 μM trimer concentration) or equimolar solutions of GlnK plus AmtB (40–43.5 μM trimers) were titrated with ATP or ADP in the presence of 0.1 or 1.0 mM 2-OG. Ligand concentrations were adjusted, according to the concentration of GlnK trimer, to obtain an optimal binding isotherm. 20 × 2-μl injections of ligand were performed with a stirring rate of 1000 rpm. Buffer conditions were 50 mM Tris-HCl (pH 7.5), 200 mM KCl, 10 mM $MgCl_2$, 10% (v/v) glycerol, and 0.03% (w/v) *n*-dodecyl-β-D-maltoside. Dissociation constants were obtained by fitting the data to a sequential binding site model, assuming existence of three sites, using the Origin 7 software supplied by MicroCal. Final data were obtained from at least two independent experiments.

Purification of GlnK for ITC—Strain BL21(DE3)pLysS pJT25 was grown in 20 ml of LB broth supplemented with 100 μg/ml carbenicillin for 8 h at 37 °C. This culture was inoculated into 1 liter of autoinduction medium (ForMedium Ltd.); grown overnight at 37 °C; harvested at 6000 × *g*; and resuspended in 50 mM Tris-HCl (pH 7.5), 100 mM KCl, and 20% glycerol. Whole cell extracts of the culture were heated to 80 °C for 4 min, cooled on ice for 10 min, and harvested by centrifugation at 28,000 × *g*. The supernatant was loaded onto a 5-ml HiTrap heparin HC column (GE Healthcare), equilibrated with 50 mM Tris-HCl (pH 7.5) and 100 mM KCl, and run at 1 ml/min. GlnK was eluted with 50 mM Tris-HCl (pH 7.5) and 1 M KCl at 2 ml/min using a two-step gradient (15 ml, 5%; and 25 ml, 10%). Pure fractions of GlnK were identified on 12.5% SDS-polyacrylamide gel and stored at −80 °C.

RESULTS

AmtB and GlnK Protein Quantification—Previous analysis of the AmtB-GlnK complex purified directly from *E. coli* cells revealed an AmtB:GlnK stoichiometry of 1:1 (15), but the *in vivo* cellular levels of GlnK and AmtB have not been determined. Our Western blotting quantification of ET8000 samples gave values of 1353 ± 255 AmtB molecules of trimer/cell (2.7 ± 0.5 ng of AmtB/μg of total cell protein) and 11,387 ± 2398 GlnK molecules of trimer/cell (6.7 ± 1.4 ng of GlnK/μg of total cell protein). Thus, the *in vivo* stoichiometric ratio of AmtB to GlnK is ~1:8 in *E. coli*.

Conditions for GlnK Membrane Sequestration—To define a set of conditions in which a complete *in vivo* cycle of AmtB-GlnK complex formation and dissociation occurs, we examined a range of ammonium concentrations added to nitrogen-limited cells. We determined that an extracellular NH_4Cl concentration of 200 μM triggered relatively rapid (30 s) membrane sequestration of GlnK (Fig. 1*A*). The highest level of membrane-bound GlnK was found at 2 min post-ammonium shock, and within 15 min, gradual ammonia assimilation elicited complete AmtB-GlnK complex dissociation. The levels of AmtB in the membrane remained constant both pre- and post-ammonium shock (Fig. 1*A*). An ammonium concentration of 200 μM and a time frame of 15 min were used in all subsequent experiments.

In Vivo Uridylylation and Deuridylylation of GlnK upon Ammonium Shock—We monitored the uridylylation status of GlnK following an ammonium shock of 200 μM. As expected, prior to the shock, GlnK was fully uridylylated. Deuridylylation of GlnK occurred within 2 min, followed by slow reuridylylation of GlnK within 15 min (Fig. 1*B*). GlnK deuridylylation/uridylylation events coincided with the membrane association status of GlnK (Fig. 1, compare *A* and *B*) such that formation of the AmtB-GlnK complex was directly proportional to the amount of GlnK deuridylylation.

In Vivo Pools of 2-OG, ATP, and ADP in Pre- and Post-ammonium-shocked Cells—A number of studies have suggested that *in vivo* formation of an AmtB-P_{II} complex is influenced by the intracellular pools of MgATP, ADP, and 2-OG metabolites (15–17, 23). To establish the relationship between these metabolites and the cellular nitrogen status, we determined the intracellular pools of ATP, ADP, and 2-OG in *E. coli* over a period of 15 min following a 200 μM ammonium shock.

In nitrogen-limited ET8000 cells, the intracellular pool of 2-OG was ~1.4 mM. However, it was rapidly depleted upon

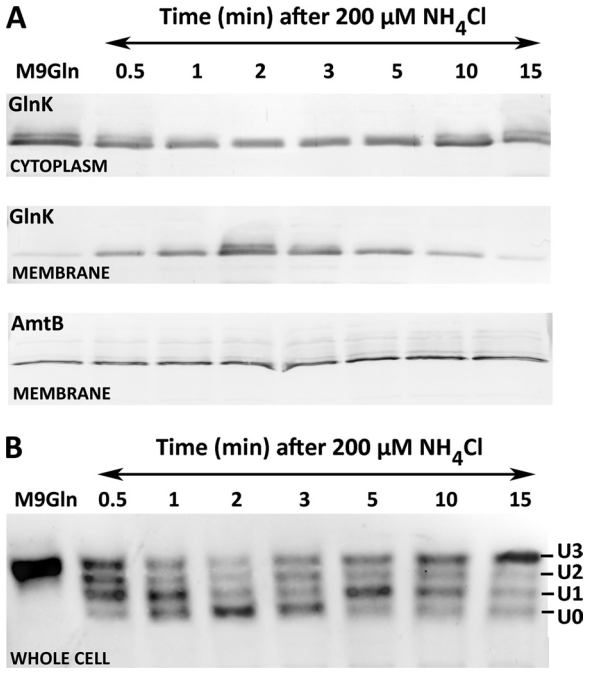

FIGURE 1. **Response of GlnK to ammonium shock.** *A*, membrane sequestration of GlnK by AmtB. 200 μM NH_4Cl was added at t_0 to a culture of *E. coli* strain ET8000 growing under nitrogen limitation (M9Gln medium), and samples were taken at the times shown. *B*, reversible uridylylation/deuridylylation of GlnK following the same treatment. Membrane and cytoplasmic fractions (*A*) were analyzed by 12.5% SDS-PAGE, and whole cell extracts (*B*) were analyzed by native 12.5% PAGE. Gels were subjected to Western blotting with anti-GlnK antibodies (*A* and *B*) and anti-AmtB antibodies (*A*).

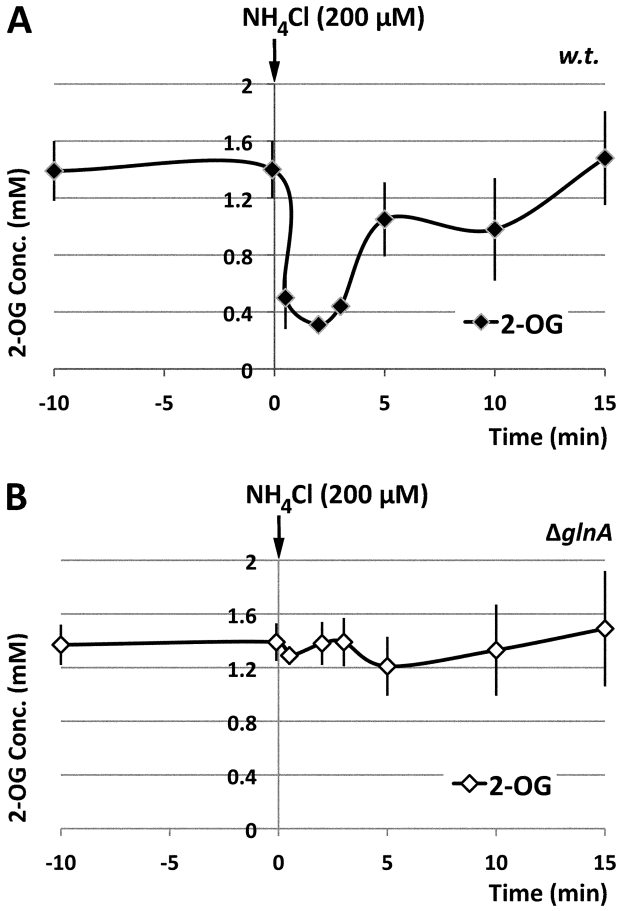

FIGURE 2. **Measurements of the *in vivo* 2-OG pool.** The experimental conditions were identical to those described in the legend to Fig. 1, but data were collected for both wild-type *E. coli* ET8000 (*A*) and a Δ*glnA* mutant strain, ET8009 (*B*). The ammonium shock was applied at 0 min as indicated by the *arrows*. The data are the average of at least four independent experiments.

addition of ammonium and, after 2 min, was reduced to 0.3 mM. Due to ammonium utilization, this rapid depletion was followed by a gradual increase in 2-OG concentration, and within 15 min, the 2-OG pool had reverted to the original level prior to ammonium shock (Fig. 2*A*).

The ATP and ADP pools of ET8000 cells were stable prior to ammonium shock (Fig. 3*A*), and the averages for two separately prepared extracts from each of at least four different cultures were 2.1 ± 0.5 mM for ATP and 0.3 ± 0.1 mM for ADP. Two significant changes in adenine nucleotide pools took place in post-ammonium-shocked cells. The first change happened within 2 min after introduction of ammonium. Fig. 3*A* shows that 30 s after ammonium addition, the ATP pool had decreased to 1.8 ± 0.5 mM, whereas the amount of ADP had increased reciprocally to 0.6 ± 0.1 mM. This change was transitory because 2 min later, the ATP and ADP levels were restored to values close to the levels of pre-ammonium-shocked ET8000 cells. The second change in ATP/ADP pools happened more gradually. A progressive increase was observed in both pools as the added ammonium was gradually metabolized. By 15 min, there was a 2-fold increase in both the ATP and ADP pools (Fig. 3*A*).

Comparison of these *in vivo* changes in effector pools with the concomitant changes in GlnK localization revealed that the membrane sequestration of GlnK by AmtB coincided with an ~5-fold decrease in the 2-OG pool, a slight decrease in the ATP pool, and an ~2-fold increase in the ADP pool, changing the ATP/ADP ratio from ~7 to ~3 within 30 s. The subsequent dissociation of the AmtB-GlnK complex occurred as the 2-OG level slowly returned to the pre-ammonium shock level, during which time there was an ~2-fold increase in ATP and ADP pools, changing the ATP/ADP ratio back to ~7–8.

2-OG, ATP, and ADP Pools in a glnA Mutant—A rapid reduction in the cellular ATP pool of *E. coli* following ammonium shock was reported in a previous study (33). It was suggested that this drop was due to the transiently elevated activity of glutamine synthetase following the increased uptake of ammonium and that the ammonium-induced inactivation of glutamine synthetase by adenylylation is necessary to protect the cell from an unsustainable drain on the ATP pool (33, 34). However, others have argued that the primary function of glutamine synthetase adenylylation is to protect the cellular glutamate pool and that other mechanisms exist to protect the ATP pool (35).

To investigate whether glutamine synthetase played a role in the observed changes in ATP and ADP pools, we analyzed the same effector pools in an *E. coli glnA* mutant (strain ET8009) that had been subjected to an identical ammonium shock. As expected, given the defective glutamine synthetase/glutamate synthase ammonium assimilation pathway in this strain, the 2-OG pool remained unchanged at 1.4 mM after ammonium shock (Fig. 2*B*). Likewise, the gradual increase in the ATP and ADP pools following ammonium influx was also dependent on

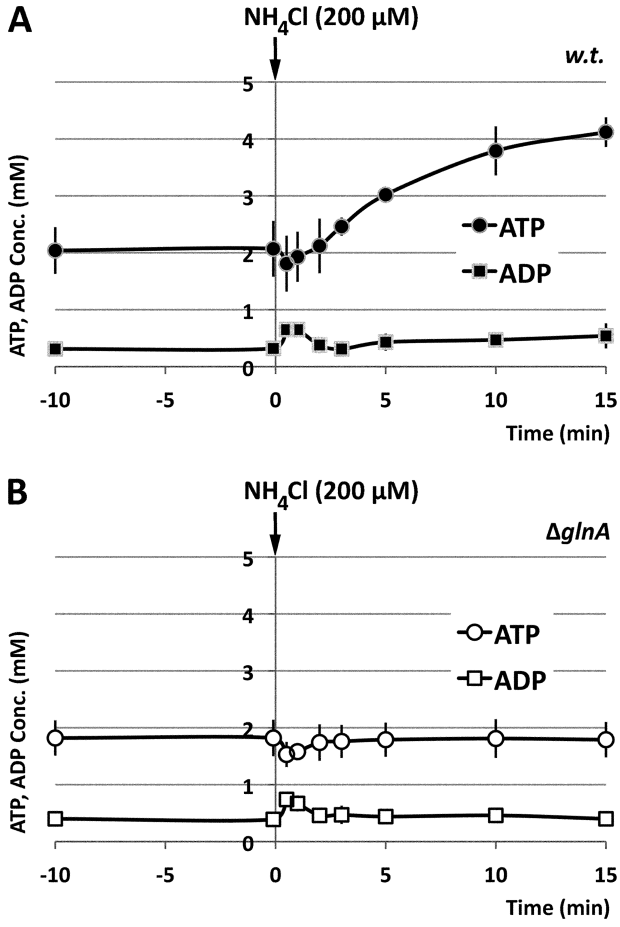

FIGURE 3. **Measurements of *in vivo* adenosine nucleotide pools.** The experimental conditions and strains used were as described in the legend to Fig. 2. The data represent concentrations of ATP and ADP (mM) at each time point and are the average of four independent experiments.

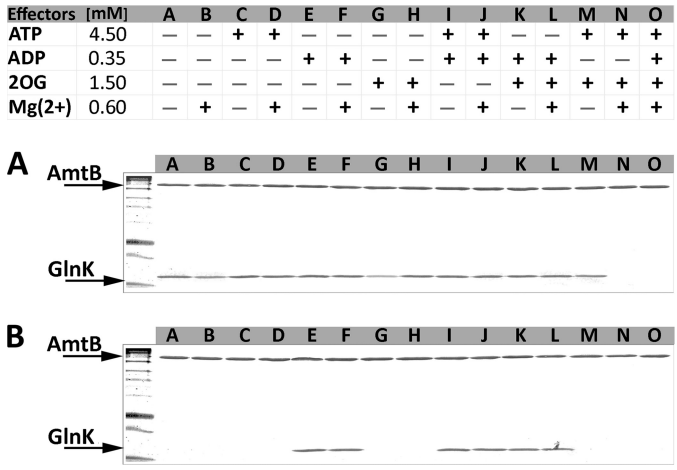

FIGURE 4. **Effects of ATP, ADP, 2-OG, and Mg^{2+} on the association and dissociation of the AmtB-GlnK complex.** Proteins were applied to a HIS-Select spin column in the presence of different combinations of effectors as listed in the *table*. In each case, the proteins retained on the column after washing were eluted and analyzed by 12.5% SDS-PAGE. *A*, to assess dissociation, purified His_6-AmtB-GlnK complex was applied to the spin column. The absence of GlnK on the gel indicates complex dissociation. *B*, to assess association, His_6-AmtB and GlnK (at a molar ratio of 1:3) were applied to the spin column. The presence of GlnK on the gel indicates complex formation.

ammonium assimilation by glutamine synthetase (Fig. 3*B*). However, the transient fluctuation in the intracellular levels of ATP and ADP that occurred within the first 2 min after ammonium shock could not be attributed to glutamine synthetase activity because strain ET8009 showed a similar profile to the wild type (Fig. 3, compare *A* and *B*).

AmtB-GlnK Complex Association/Dissociation in Vitro—Having established the *in vivo* concentrations of different effectors during the association/dissociation cycle, we examined whether the apparent effects of the *in vivo* fluctuations could be replicated *in vitro*. In selecting concentrations of effectors to use in these *in vitro* studies, we were guided by the intracellular concentrations determined *in vivo*.

Initially, we examined the effects of ATP, ADP, or 2-OG individually and in combinations on both association and dissociation of the AmtB-GlnK complex. Dissociation of the preformed complex was observed only when both MgATP and 2-OG were present (Fig. 4*A*, *lanes N* and *O*). Conversely, association of GlnK and AmtB was completely dependent on the presence of ADP (Fig. 4*B*, *lanes E*, *F*, and *I–L*) unless high 2-OG and MgATP were also present (*lane O*). In a previous study (15), we reported that ATP was sufficient to promote complex formation. However, in those experiments, we preincubated the proteins with the effectors for 15 min at 30 °C. It has been reported that preparation of P_{II} proteins is prone to ATPase contamination (36). We therefore consider that our previous observations were due to hydrolysis of ATP to ADP by an ATPase contaminant.

ATP and ADP are expected to compete because they share the same GlnK-binding site, and consequently, the ATP/ADP ratio could have a significant effect on association or dissociation. Hence, we examined the effects of the extreme ADP concentrations determined in our *in vivo* studies (0.35 and 0.75 mM) combined with either high (1.5 mM) or low (0.3 mM) 2-OG and either high (4.5 mM) or low (2 mM) ATP (Fig. 5).

ADP had a very significant impact on the stability of the preformed AmtB-GlnK complex. The presence of 0.75 mM ADP completely prevented dissociation, even in the presence of high concentrations of 2-OG and ATP, which would otherwise promote dissociation both *in vitro* and *in vivo* (Fig. 5*A*, *lanes A–D*). However, at 0.35 mM ADP, dissociation was effectively determined by the 2-OG concentration (Fig. 5*A*, *lanes E–H*). By contrast, when association of the individual proteins was examined, the dominant effector was a high concentration of 2-OG (1.5 mM) (Fig. 5*B*, *lanes A*, *B*, *E*, and *F*). When the concentration of 2-OG was low (0.3 mM), the presence of ADP was sufficient to promote complex formation, although 0.75 mM ADP was notably more effective than 0.3 mM ADP (Fig. 5*B*, *lanes C*, *D*, *G*, and *H*).

We then examined whether the specific combinations of intracellular effector concentrations measured *in vivo* would replicate *in vitro* the association or dissociation of the complex. Starting with the purified complex, we were able to re-enact the intracellular events that led to complex dissociation within 15 min after ammonium shock (Fig. 6*A*). Complex dissociation began at the equivalent of the 3-min time point, and the gradual increase in 2-OG and ATP led to complete AmtB-GlnK dissociation (Fig. 6*A*). Conversely, by starting with the individual proteins and using identical combinations of effector concentrations, we were able to re-enact the intracellular events that

Effectors	[mM]	A	B	C	D	E	F	G	H
ATP	4.50	–	+	+	–	–	+	+	–
ATP	2.00	+	–	–	+	+	–	–	+
ADP	0.75	+	+	+	+	–	–	–	–
ADP	0.35	–	–	–	–	+	+	+	+
2-OG	1.50	+	+	–	–	+	+	–	–
2-OG	0.30	–	–	+	+	–	–	+	+

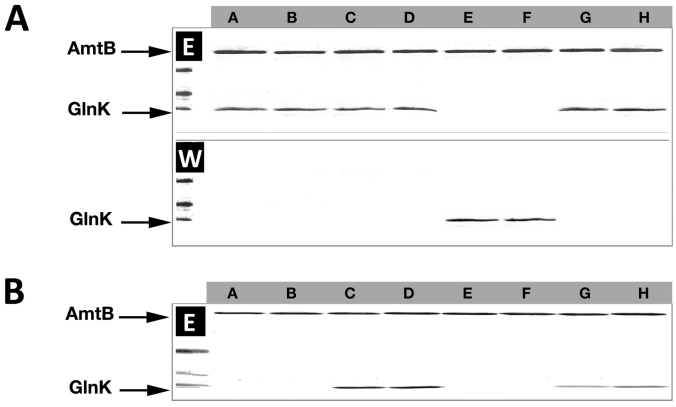

FIGURE 5. **Effects of varying ADP concentrations on the stability of the AmtB-GlnK complex.** *A*, purified His_6-AmtB-GlnK complex was applied to a HIS-Select spin column in the presence of different combinations of effectors as listed in the *table*. Washed and eluted fractions were analyzed by 12.5% SDS-PAGE. The presence of GlnK in the washed fractions (*W*) indicates conditions under which GlnK dissociated from AmtB. Conversely, GlnK in the eluted fractions (*E*) indicates that the His_6-AmtB-GlnK complex remained associated. *B*, AmtB and GlnK proteins were applied separately to the column. The presence of GlnK in the eluted fractions indicates conditions under which GlnK associated with AmtB.

led to complex association. AmtB-GlnK association was optimized by a low ATP/ADP ratio (<6.0) combined with a low 2-OG concentration (0.3–0.4 mM) (Fig. 6*B*).

E. coli GlnK-Ligand Binding Constants Determined by Isothermal Calorimetry—One of the major factors in determining the effects of fluctuating intracellular ligand concentrations on the behavior of GlnK is the affinity of the protein for these ligands alone or in combination. We used ITC to determine the binding constants of *E. coli* GlnK for ATP and ADP in the presence of high (1 mM) and low (0.1 mM) concentrations of 2-OG (Fig. supplemental S1, *A*, *B*, *D*, and *E*). Furthermore, because complex formation between GlnK and AmtB occurs only at low 2-OG, we also examined binding of both ATP and ADP to GlnK in the presence of low 2-OG and AmtB (Table 1 and supplemental Fig. S1, *C* and *F*).

Under all of the conditions, the best fit to the data was obtained using a model with three classes of binding sites. Binding of ATP to GlnK was ~11-fold greater in the presence of high 2-OG compared with low 2-OG (Table 1 and supplemental Fig. S1, *A* and *B*). Binding of ADP to GlnK showed reciprocal properties to ATP, being 4-fold less in the presence of high 2-OG compared with low 2-OG (Table 1 and supplemental Fig. S1, *D* and *E*). The presence of AmtB had no marked effect on binding of ADP or ATP (Table 1 and supplemental Fig. S1, *C* and *F*).

When the 2-OG concentration was high, ATP had an 8-fold greater affinity for GlnK compared with ADP, whereas at low 2-OG, ADP had a 5-fold greater affinity compared with ATP (Table 1 and supplemental Fig. S1). Examination of the total Gibbs free energy (ΔG) is consistent with this pattern. At high

Effectors	[mM]	A	B	C	D	E	F	G
2-OG	0.3	–	–	+	–	–	–	–
2-OG	0.4	+	+	–	+	–	–	–
2-OG	1	–	–	–	–	+	+	–
2-OG	1.5	–	–	–	–	–	–	+
ATP	2	+	+	+	–	–	–	–
ATP	2.6	–	–	–	+	–	–	–
ATP	3.3	–	–	–	–	+	–	–
ATP	4	–	–	–	–	–	+	–
ATP	4.5	–	–	–	–	–	–	+
ADP	0.3	+	–	–	+	–	–	–
ADP	0.4	–	–	+	–	–	–	–
ADP	0.5	–	–	–	–	+	+	–
ADP	0.6	–	+	–	–	–	–	+

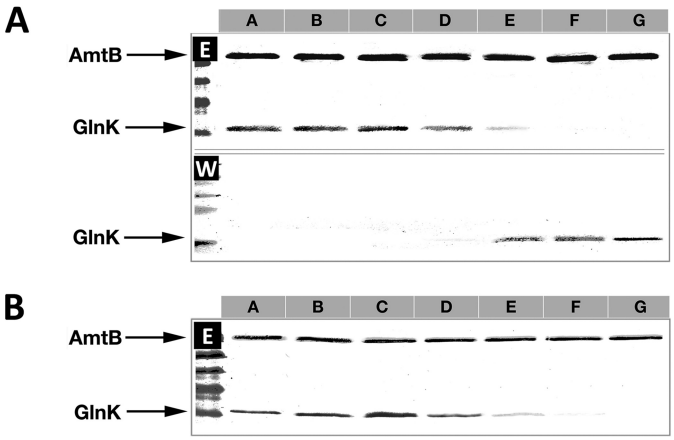

FIGURE 6. **Interactions between AmtB and GlnK in response to physiologically relevant concentrations of ATP, ADP, 2-OG, and Mg^{2+} effectors.** *A*, purified His_6-AmtB-GlnK complex was applied to a HIS-Select spin column in the presence of different combinations of effectors. The effector concentrations used reflect the measured *in vivo* values at 30 s, 1 min, 2 min, 3 min, 5 min, 10 min, and 15 min post-ammonium shock (*lanes A–G*). Washed and eluted fractions were analyzed by 12.5% SDS-PAGE. The presence of GlnK in the washed fractions (*W*) indicates conditions under which GlnK dissociated from AmtB. Conversely, GlnK in the eluted fractions (*E*) indicates that the His_6-AmtB-GlnK complex remained associated. *B*, individual AmtB and GlnK proteins were applied to the column. The presence of GlnK in the eluted fractions indicates conditions under which GlnK associated with AmtB.

TABLE 1

Thermodynamic parameters of ATP and ADP binding to *E. coli* GlnK

For both ATP and ADP, experiments were performed in the presence of high 2-OG (1 mM), low 2-OG (0.1 mM), and low 2-OG plus AmtB. Gibbs energy (ΔG) values for each binding site were calculated using $\Delta G = -RT\ln K_a = \Delta H - T\Delta S$ (data not shown). The ΔG values are the sum of the values for all three sites.

Binding molecule	K_{d1}	K_{d2}	K_{d3}	ΔG
	μM	μM	μM	kcal/mol
ATP				
GlnK/2-OG (1 mM)	7.2 ± 0	28.9 ± 3.4	141.3 ± 41.1	−18.7 ± 0.2
GlnK/2-OG (0.1 mM)	81.2 ± 6.1	36.2 ± 2.3	326.0 ± 76.7	−16.6 ± 0.2
GlnK/AmtB/2-OG (0.1 mM)	45.5 ± 16.4	145.6 ± 129.1	101.3 ± 28.3	−16.7 ± 0.8
ADP				
GlnK/2-OG (1 mM)	56.9 ± 11.4	135.9 ± 30.2	347.1 ± 48.9	−16.0 ± 0.3
GlnK/2-OG (0.1 mM)	14.9 ± 6.9	90.3 ± 25.1	377.5 ± 16.3	−17.0 ± 0.3
GlnK/AmtB/2-OG (0.1 mM)	8.9 ± 0.4	21.4 ± 20.4	147.5 ± 164.5	−19.1 ± 1.6

2-OG and in the absence of AmtB, formation of the GlnK-ATP complex was favored compared with GlnK-ADP by 2.7 kcal/mol, whereas at low 2-OG and in the presence of AmtB, the reciprocal situation pertained, with formation of the AmtB-GlnK-ADP complex favored by 2.4 kcal/mol (Table 1).

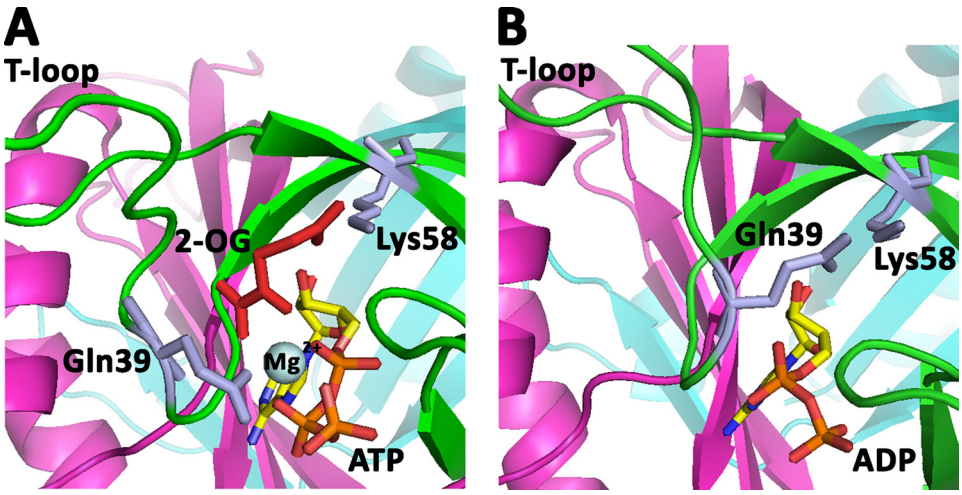

FIGURE 7. **Comparison of the structures of the P_{II} ligand-binding site.** *A*, the equivalent of nitrogen-sufficient conditions when P_{II} is not complexed with AmtB (*A. brasilense* GlnZ with 2-OG and MgATP bound; Protein Data Bank code 3MHY). *B*, nitrogen-limited conditions when the AmtB-P_{II} complex is formed (*E. coli* GlnK with ADP bound and complexed with AmtB; Protein Data Bank code 2NUU).

These data for *E. coli* GlnK are largely consistent with similar studies of ligand binding to *E. coli* GlnB, which was assessed using an alternative technique (16). GlnB also shows negative cooperativity of ATP binding and synergistic binding of ATP and 2-OG. However, unlike our data for GlnK, ADP binding to GlnB was not suggestive of multiple classes of sites and was also not influenced by the presence of 2-OG.

DISCUSSION

It has long been recognized that the interactions of P_{II} proteins with their targets are controlled by changes in the intracellular concentrations of key metabolites: ATP, ADP, and 2-OG (12, 20). However, the manner in which these metabolites interact to regulate the association and dissociation of P_{II} and its targets has not been understood at the molecular level for any P_{II} complex. In this study, we have determined *in vivo* fluctuations in effector levels as they occur in concert with association and dissociation of a specific P_{II} complex. By combining this with *in vitro* studies and recent knowledge of how 2-OG binds to P_{II} proteins, we have been able to develop a model that explains the signal transduction process that underlies AmtB-GlnK complex formation and dissociation.

Changes in GlnK Effector Concentrations—The inherent difficulties in measuring intracellular effector concentrations, in particular with regard to nucleotide pools, are well documented (37–39). It is also not possible to distinguish free and macromolecule-bound metabolites. However, given that the measured total metabolome concentration of 300 mM greatly exceeds the reported total protein concentration of 7 mM (40), it is likely that our measured values largely reflect free metabolites. Furthermore, our ability to replicate *in vitro* quite accurately the behavior of GlnK with regard to its interaction with AmtB, by using our calculated intracellular effector concentrations, provides a robust validation of our *in vivo* analyses.

The very significant and rapid drop that we observed in the 2-OG pool within 1 min of ammonium shock (Fig. 2) agrees well with a recent metabolomic study (34) and with the previously reported reciprocal rise in the glutamine pool (33, 34). As AmtB-GlnK complex formation occurs *in vitro* only at a low 2-OG concentration (0.1 mM), this drop in the 2-OG pool appears to be a major factor facilitating GlnK sequestration by AmtB. However, the highly conserved property of P_{II} proteins to bind ATP or ADP and the observation that, in the AmtB-GlnK complex purified directly from ammonium-shocked cells, all the nucleotide-binding sites of GlnK are occupied by ADP, clearly implicate ATP/ADP binding as also playing a key role. Previous studies of ATP/ADP pools following ammonium shock of nitrogen-limited cells have produced varied results, ranging from a very rapid drop in the intracellular ATP pool (33) to no detectable fluctuation in nucleotide pools (34, 39). However, the culture conditions and the sampling methods used in all of those experiments were quite different from those used in this study.

The high affinity of P_{II} proteins for ATP (K_{d1} in the range of 1–50 μM) (21) previously led to the view that, given intracellular ATP concentrations between 2 and 5 mM, ATP could play no regulatory role *in vivo* (41). However, it has recently been determined that, in *E. coli*, the concentration of ATP typically exceeds the K_m values for enzymes to which it binds by >10-fold (40). Indeed, the absolute concentrations of >100 metabolites in *E. coli* exceed the relevant K_m values for most substrate-enzyme pairs (40). Nevertheless, it has been proposed that, in such cases, competition for binding at active sites can still allow sensitivity of flux to substrate concentration (34, 40). Conceivably, a similar rationale (in this case, competition between ATP and ADP for binding to P_{II}) might explain how these signal transduction proteins achieve responsiveness to relatively small changes in nucleotide pools.

In our study, a significant feature is the transient drop in the ATP/ADP ratio from ~7.0 to nearly 3.0 at the same time that the intracellular 2-OG concentration drops by 5-fold (compare Figs. 2*A* and 3*A*). Our *in vitro* studies emphasized the antagonistic effects of ADP and 2-OG in controlling complex association/dissociation. Furthermore, our ITC studies (Table 1 and supplemental Fig. S1) and other assessments of GlnK-ligand interactions (21) show that the affinity of GlnK for ATP is significantly reduced when the availability of 2-OG is low. Consequently, given the synergy of 2-OG and ATP binding, a drop in 2-OG together with a simultaneous decrease in the ATP/ADP ratio will facilitate competition between ADP and ATP, leading to replacement of 2-OG and MgATP by ADP.

The key role of 2-OG in this signal transduction process is likely to be common to interactions of P_{II} proteins with most (if not all) of their targets. However, for regulation of AmtB-GlnK complex formation, the antagonistic effect of ADP on 2-OG binding also appears to be critical. Many authors have proposed

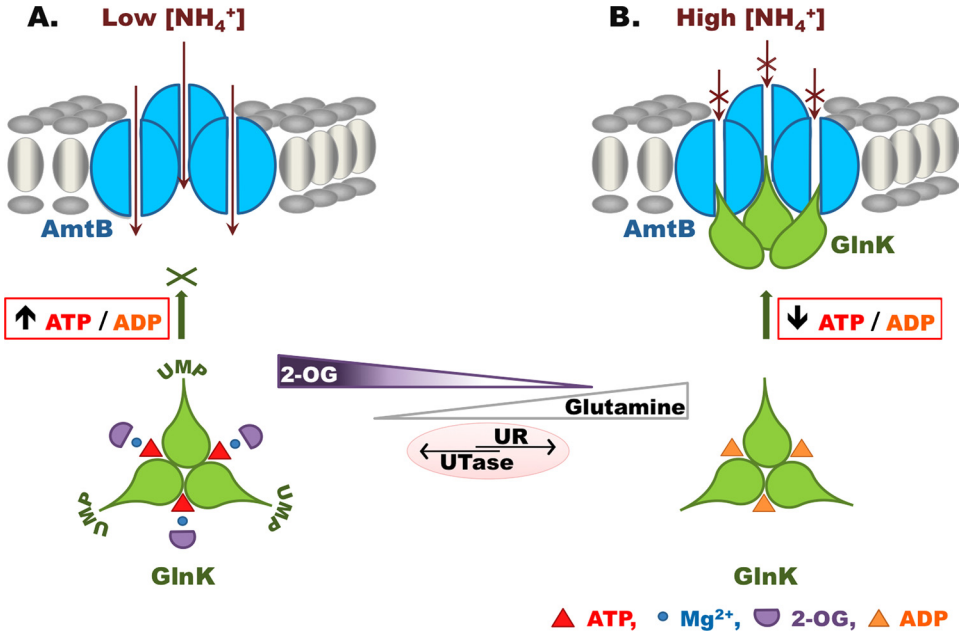

FIGURE 8. **Model describing the role of the GlnK effectors (ATP, ADP, Mg^{2+}, and 2-OG) in regulating complex formation between GlnK and AmtB.** *A*, when the extracellular ammonium concentration is low, the intracellular glutamine level is also low, leading to a high uridylyltransferase (*UTase*) activity of GlnD. The intracellular 2-OG concentration is high, and the ATP/ADP ratio is high. Under these conditions, ATP, Mg^{2+}, and 2-OG are bound to GlnK, which is fully uridylylated and unable to form a complex with AmtB. *B*, a rise in extracellular ammonium results in an increase in the intracellular glutamine concentration due to the activity of glutamine synthetase. The increased glutamine pool promotes deuridylylation of GlnK by the uridylyl-removing (*UR*) activity of GlnD. There is also a concomitant fall in the 2-OG pool and a transient decrease in the intracellular ATP/ADP ratio. As a consequence, GlnK is fully deuridylylated, its 2-OG-binding site is unoccupied, and MgATP is replaced by ADP. These changes favor complex formation with AmtB, which is completely reversible. As the cellular nitrogen status falls again and the 2-OG pool increases, MgATP and 2-OG can replace ADP on GlnK, leading to its dissociation from AmtB.

that P_{II} proteins can sense changes in adenylate charge (16, 21, 42, 43). However, adenylate charge (defined as [ATP] + ½[ADP]/[ATP + ADP + AMP]) is apparently strongly buffered around a value of 0.9 or greater (40, 44), and our data are consistent with this. Consequently, it remains to be established whether there is a common underlying physiological link between the ATP/ADP ratio and regulation of P_{II} interactions with specific targets.

How Changes in Effector Pools Influence GlnK Structure—The recent description of a high-resolution x-ray structure for the GlnZ protein of *A. brasilense* with bound 2-OG and MgATP provides a critical insight into the interactions of these key effectors with P_{II} proteins (24). GlnZ is the *A. brasilense* ortholog of *E. coli* GlnK and regulates *A. brasilense* AmtB in an equivalent fashion (18), so we have used the new GlnZ structure to predict how changes in effector pools will influence the conformation of GlnK and facilitate its binding to AmtB.

When GlnK is dissociated from AmtB, it is bound by ATP and 2-OG, both of which participate in coordination of Mg^{2+}, for which they provide five oxygen ligands; the sixth ligand is provided by the conserved P_{II} residue Gln^{39} (Fig. 7*A*) (24). The 5-carboxyl group of 2-OG also forms a salt bridge with the ammonium group of the conserved P_{II} residue Lys^{58} (Fig. 7*A*). By comparison, when GlnK is complexed with AmtB, ADP replaces 2-OG and MgATP, and Gln^{39} moves to occupy the space vacated by 2-OG, thereby substituting the interaction of 2-OG with Lys^{58} (Fig. 7*B*) (23). Gln^{39} and Lys^{58} are both located near the base of the T-loop, and hence, a consequence of this rearrangement will be a change in the conformation of the T-loop. The presence of ADP presumably reduces the conformational space of the T-loop, thereby favoring the novel extended conformation that promotes interaction with AmtB (23). Once the AmtB-GlnK complex has formed, the key to dissociation appears to be the concomitant increase in the 2-OG and ATP pools that occurs as a result of the elevated cellular nitrogen status. As the ATP/ADP ratio returns to ~7 and the 2-OG pool approaches the initial concentration of ~1 mM, the equilibrium between binding of ADP or MgATP changes, and the original 2-OG/MgATP-bound form of GlnK is restored. Furthermore, dissociation of the T-loop will render Tyr^{51} accessible to uridylyltransferase, so GlnK becomes progressively uridylylated. This covalent modification of GlnK, which is not a feature of all P_{II} proteins, will likely prevent further interaction with AmtB until a rise in the intracellular glutamine pool again signals nitrogen sufficiency and directly activates the uridylyl-removing activity of GlnD. This model, which could serve as a basis for understanding the regulatory properties of other P_{II} proteins, is summarized in Fig. 8.

Future studies of the ways in which effector pools fluctuate in other systems, *e.g.* the interaction of P_{II} proteins with *N*-acetylglutamate kinase (45, 46), should allow us to develop a more comprehensive understanding of the mode of action of these remarkable signal transduction proteins.

Acknowledgments—We thank Simon Andrews for providing E. coli strain JW3841 (ECK3863); Ray Dixon, Luciano Huergo, and Fritz Winkler for helpful discussions and comments on the manuscript; Richard Little and Verity Lyall for advice on ITC; and Geoff Plumb for help with ATP/ADP analysis.

REFERENCES

1. von Wirén, N., and Merrick, M. (2004) *Trends Curr. Genet.* **9,** 95–120
2. Liu, Z., Peng, J., Mo, R., Hui, C., and Huang, C. H. (2001) *J. Biol. Chem.* **276,** 1424–1433
3. Merrick, M., Javelle, A., Durand, A., Severi, E., Thornton, J., Avent, N. D., Conroy, M. J., and Bullough, P. A. (2006) *Transfus. Clin. Biol.* **13,** 97–102
4. Javelle, A., Thomas, G., Marini, A. M., Krämer, R., and Merrick, M. (2005) *Biochem. J.* **390,** 215–222
5. Zheng, L., Kostrewa, D., Bernèche, S., Winkler, F. K., and Li, X. D. (2004) *Proc. Natl. Acad. Sci. U.S.A.* **101,** 17090–17095
6. Thornton, J., Blakey, D., Scanlon, E., and Merrick, M. (2006) *FEMS Microbiol. Lett.* **258,** 114–120
7. Khademi, S., O'Connell, J., 3rd, Remis, J., Robles-Colmenares, Y., Miercke, L. J., and Stroud, R. M. (2004) *Science* **305,** 1587–1594

8. Javelle, A., Lupo, D., Ripoche, P., Fulford, T., Merrick, M., and Winkler, F. K. (2008) *Proc. Natl. Acad. Sci. U.S.A.* **105,** 5040–5045
9. Javelle, A., Lupo, D., Zheng, L., Li, X. D., Winkler, F. K., and Merrick, M. (2006) *J. Biol. Chem.* **281,** 39492–39498
10. Thomas, G., Coutts, G., and Merrick, M. (2000) *Trends Genet.* **16,** 11–14
11. Sant'Anna, F. H., Trentini, D. B., de Souto Weber, S., Cecagno, R., da Silva, S. C., and Schrank, I. S. (2009) *J. Mol. Evol.* **68,** 322–336
12. Forchhammer, K. (2008) *Trends Microbiol.* **16,** 65–72
13. Javelle, A., Severi, E., Thornton, J., and Merrick, M. (2004) *J. Biol. Chem.* **279,** 8530–8538
14. Coutts, G., Thomas, G., Blakey, D., and Merrick, M. (2002) *EMBO J.* **21,** 536–545
15. Durand, A., and Merrick, M. (2006) *J. Biol. Chem.* **281,** 29558–29567
16. Teixeira, P. F., Jonsson, A., Frank, M., Wang, H., and Nordlund, S. (2008) *Microbiology* **154,** 2336–2347
17. Wolfe, D. M., Zhang, Y., and Roberts, G. P. (2007) *J. Bacteriol.* **189,** 6861–6869
18. Huergo, L. F., Merrick, M., Pedrosa, F. O., Chubatsu, L. S., Araujo, L. M., and Souza, E. M. (2007) *Mol. Microbiol.* **66,** 1523–1535
19. Yildiz, O., Kalthoff, C., Raunser, S., and Kühlbrandt, W. (2007) *EMBO J.* **26,** 589–599
20. Ninfa, A. J., and Jiang, P. (2005) *Curr. Opin. Microbiol.* **8,** 168–173
21. Jiang, P., and Ninfa, A. J. (2007) *Biochemistry* **46,** 12979–12996
22. Xu, Y., Cheah, E., Carr, P. D., van Heeswijk, W. C., Westerhoff, H. V., Vasudevan, S. G., and Ollis, D. L. (1998) *J. Mol. Biol.* **282,** 149–165
23. Conroy, M. J., Durand, A., Lupo, D., Li, X. D., Bullough, P. A., Winkler, F. K., and Merrick, M. (2007) *Proc. Natl. Acad. Sci. U.S.A.* **104,** 1213–1218
24. Truan, D., Huergo, L. F., Chubatsu, L. S., Merrick, M., Li, X. D., and Winkler, F. K. (2010) *J. Mol. Biol.* **400,** 531–539
25. Gruswitz, F., O'Connell, J., 3rd, and Stroud, R. M. (2007) *Proc. Natl. Acad. Sci. U.S.A.* **104,** 42–47
26. MacNeil, D. (1981) *J. Bacteriol.* **146,** 260–268
27. Baba, T., Ara, T., Hasegawa, M., Takai, Y., Okumura, Y., Baba, M., Datsenko, K. A., Tomita, M., Wanner, B. L., and Mori, H. (2006) *Mol. Syst. Biol.* **2,** 1–11
28. Datsenko, K. A., and Wanner, B. L. (2000) *Proc. Natl. Acad. Sci. U.S.A.* **97,** 6640–6645
29. Studier, F. W., Rosenberg, A. H., Dunn, J. J., and Dubendorff, J. W. (1990) *Methods Enzymol.* **185,** 60–89
30. Tabor, S., and Richardson, C. C. (1985) *Proc. Natl. Acad. Sci. U.S.A.* **82,** 1074–1078
31. Forchhammer, K., Hedler, A., Strobel, H., and Weiss, V. (1999) *Mol. Microbiol.* **33,** 338–349
32. Reyes-Ramirez, F., Little, R., and Dixon, R. (2001) *J. Bacteriol.* **183,** 3076–3082
33. Schutt, H., and Holzer, H. (1972) *Eur. J. Biochem.* **26,** 68–72
34. Yuan, J., Doucette, C. D., Fowler, W. U., Feng, X. J., Piazza, M., Rabitz, H. A., Wingreen, N. S., and Rabinowitz, J. D. (2009) *Mol. Syst. Biol.* **5,** 302
35. Kustu, S., Hirschman, J., Burton, D., Jelesko, J., and Meeks, J. C. (1984) *Mol. Gen. Genet.* **197,** 309–317
36. Jiang, P., and Ninfa, A. J. (1999) *J. Bacteriol.* **181,** 1906–1911
37. Schneider, D. A., and Gourse, R. L. (2004) *J. Biol. Chem.* **279,** 8262–8268
38. Rabinowitz, J. D., and Kimball, E. (2007) *Anal. Chem.* **79,** 6167–6173
39. Zhang, Y., Pohlmann, E. L., and Roberts, G. P. (2009) *J. Bacteriol.* **191,** 5526–5537
40. Bennett, B. D., Kimball, E. H., Gao, M., Osterhout, R., Van Dien, S. J., and Rabinowitz, J. D. (2009) *Nat. Chem. Biol.* **5,** 593–599
41. Kamberov, E. S., Atkinson, M. R., and Ninfa, A. J. (1995) *J. Biol. Chem.* **270,** 17797–17807
42. Jiang, P., and Ninfa, A. J. (2009) *Biochemistry* **48,** 11522–11531
43. Zhang, Y., Wolfe, D. M., Pohlmann, E. L., Conrad, M. C., and Roberts, G. P. (2006) *Microbiology.* **152,** 2075–2089
44. Chapman, A. G., Fall, L., and Atkinson, D. E. (1971) *J. Bacteriol.* **108,** 1072–1086
45. Mizuno, Y., Moorhead, G. B., and Ng, K. K. (2007) *J. Biol. Chem.* **282,** 35733–35740
46. Llácer, J. L., Contreras, A., Forchhammer, K., Marco-Marín, C., Gil-Ortiz, F., Maldonado, R., Fita, I., and Rubio, V. (2007) *Proc. Natl. Acad. Sci. U.S.A.* **104,** 17644–17649